



# Tool wear studies in fabrication of microchannels in ultrasonic micromachining



Manjot S. Cheema\*, Akshay Dvivedi, Apurbba K. Sharma

Department of Mechanical and Industrial Engineering, Indian Institute of Technology, Roorkee 247667, India

## ARTICLE INFO

### Article history:

Received 9 January 2014  
Received in revised form 4 June 2014  
Accepted 21 October 2014  
Available online 31 October 2014

### Keywords:

Ultrasonic micromachining  
Microchannels  
Tool wear  
Form accuracy

## ABSTRACT

Form accuracy of a machined component is one of the performance indicators of a machining process. Ultrasonic micromachining is one such process in which the form accuracy of the micromachined component significantly depends upon the form stability of tool. Unlike macromachining, a very small amount of tool wear in micromachining could lead to considerable changes in the form accuracy of the machined component. Appropriate selection of tool material is essential to overcome this problem. The present study discusses the effect of tool material, abrasive size and step feed in fabrication of microchannels by ultrasonic machining on borosilicate glass. Development of microchannels using ultrasonic micromachining were rarely reported. It was observed that tungsten carbide tool provided a better form accuracy in comparison to the microchannel machined by stainless steel tool. The tool wear mechanism in both materials is proposed by considering scanning electron micrographs of the tool as evidence. A one factor at a time approach was used to study the effect of various process parameters.

© 2014 Elsevier B.V. All rights reserved.

## 1. Introduction

Tool wear can be considered as one of the most important parameters which decides the form accuracy of a machined component. Form accuracy, on the other hand manifests as how close the machining process replicated the dimensions of cutting tool on the workpiece surface [1]. The efficacy of ultrasonic micromachining can also be measured by form accuracy of the machined component. As the tool gets worn out with time, a noticeable change is observed in form accuracy forcing the component towards rejection in the quality check. However, form accuracy can be achieved significantly by controlling and maintaining the tool shape and size. Tool material properties are important parameters effecting the tool wear. Maintaining form accuracy becomes even more challenging while machining at micro levels.

Flexibility and feasibility of machining micro components using ultrasonic machining (USM) have already been demonstrated [2–4]. Hard and brittle materials like glass, silicon wafers and ceramics could easily be machined by USM in the micro domain too [5]. Moreover, while compared to chemical methods of etching and lithography, USM is preferred as a cleaner and faster process. Extensive work have been reported in macro drilling of various hard and brittle materials [6]. Studies were carried out on tool

wear at macro levels. In one of the studies, the tool wear pattern was divided into two types – lateral wear and longitudinal wear [7]. Lateral wear at the tool edges occurred due to the abrasive rubbing phenomenon between the tool and workpiece walls. Lateral wear was also found responsible for reduction in tool diameter. On the other hand, longitudinal wear was responsible in reduction of tool length which occurred due to microchipping and cavitation phenomenon [8]. The complete tool wear during USM of macro holes was thus, a combination of both the wear patterns. Some researchers reported that with an increase in machining time, microhardness of the tool was found to be more at the edges in comparison to the middle part. Plastic flow and work hardening were found to be the major reasons for increased hardness [9].

In macro machining, if the tool gets slightly worn out, the machined product can still fall in the desired range. However, in case of machining in the micro regime, for example, fabrication of components like microchannels and microholes, the form accuracy gets affected drastically with minimal tool wear. Consequently the parts are liable to be rejected. One of the ways for achieving desired form accuracy is to minimize tool wear to the extreme possible.

Tool wear in USM mainly depends upon a number of factors like workpiece material, tool material, amplitude, applied frequency of vibration, abrasive type, abrasive size, static load and concentration of abrasive particles. Proper combination of the above mentioned parameters is essential to minimize the eventuality

\* Corresponding author.

E-mail address: [manjotcheema@hotmail.com](mailto:manjotcheema@hotmail.com) (M.S. Cheema).

wear. But the tool material is the most crucial parameter deciding the wear. Nimonic alloys, thoriated tungsten, tungsten carbide (WC), high speed steel, silver steel, titanium, maraging steel and mild steels have been the most commonly used tool materials for ultrasonic macro machining [10]. While macro drilling, it was reported that stainless steel (SS) tool is far better than WC tool [7–9,11]. This implied that SS could be an excellent candidate for ultrasonic micromachining. It is easily available and is a cost effective solution for machining. The ultrasonic micromachining can be differentiated from the macromachining by the size of machined features developed, which is generally less than 1 mm.

However, conflicting opinions were revealed for SS tool in USM at micro levels [2,3,12–14]. Some studies in ultrasonic micromachining include development of models for predicting tool wear [10].

These contradictions encouraged the present study on tool wear of SS and WC tool while fabricating microchannels on borosilicate glass. The tool wear effect on the form accuracy of developed microchannels was investigated in this study. Further, this study deals with identification of tool wear mechanism. Subsequently this article defines the type of tool material for microchannel fabrication. A one factor at a time approach was used to study the effect of step feed and abrasive size on the form accuracy of developed microchannels using SS and WC tool.

## 2. Methodology

A layer by layer machining approach was used for machining a 10 mm long microchannel using USM. In USM, a solid cylindrical tool can be used in the same method as an end mill in milling process. Cylindrical tool provided the flexibility of machining in various axis and number of profiles could be developed. In the present study SS and WC tools of same diameter were used. The experimental details are given in Table 1.

A XY axis (built in house) was used to provide motion to the borosilicate glass workpiece. The glass workpiece was mounted on a fixture. Part programming was carried out through a dedicated software of the 3 axis programmable XY stage. The XY stage had an accuracy of 0.1  $\mu\text{m}$ . Machining was completed after a number of repeated cycle with a step feed in Z axis of 5, 10 and 15  $\mu\text{m}$  in each pass. A depth of 300  $\mu\text{m}$  was achieved while using each tool material. Silicon carbide abrasive slurry (15% by weight) was kept on flowing through the tool and the workpiece gap.

The width and depth of micro channel periphery were measured at 50 $\times$  magnification on the dedicated software of microscope (Model: Dewinter DMI premium). The top view and side view of the tools were captured by a LEO scanning electron microscope (SEM), (Model: LEO 435VP). The tool images were captured by a stereo zoom microscope (Model: Nikon SMZ-745 T).

**Table 1**  
Parameters used in ultrasonic micromachining.

| Experimental conditions          |  |
|----------------------------------|--|
| Power                            | 800 W                                      |
| Vibration frequency              | 20 kHz                                     |
| Amplitude of applied vibration   | 20–30 $\mu\text{m}$                        |
| Abrasive material                | Silicon carbide                            |
| Abrasive size (mesh)             | 1800#, 1000# and 800#                      |
| Workpiece material               | Borosilicate glass                         |
| Tool material                    | (i) Tungsten carbide, (ii) stainless steel |
| Tool diameter                    | $\varnothing$ 600 $\mu\text{m}$            |
| Feed in X direction              | 30 mm/min                                  |
| Step feed in Z direction         | 5, 10, 15 $\mu\text{m}$                    |
| Total depth given in Z direction | 300 $\mu\text{m}$                          |
| Slurry medium                    | Water                                      |
| Slurry concentration             | 15% Abrasive by weight                     |

## 3. Mechanism of tool wear

In USM, when the vibrating tool goes up to the topmost position. It accumulates abrasive particles in between the tool and workpiece. The tool when comes down, strikes the abrasive particle which further strikes the workpiece. This gap created between tool and workpiece is known as the working gap (Fig. 1). The cavity (Area ABCDEF) developed during machining is always slightly bigger than the tool size owing to abrasive movement adjoining the tool surface. The gap in this enlarged cavity between the workpiece walls and the tool boundary is known as the lateral gap which is created due to the exit of abrasive particles as shown in Fig. 1. The motion of abrasive particles from working gap to lateral gap can be classified into the following three zones which exhibited different mechanisms (Fig. 1):

1. Pure hammering + cavitation (zone-1).
2. Hammering + abrasion + cavitation (zone-2).
3. Pure abrasion + rolling (zone-3).

In USM, the most dominant mode of material removal is the hammering action [6]. As the vibrating tool strikes the abrasive particles, the entire energy is transmitted to the abrasive particles. The abrasive particles further strike the workpiece material causing microcracks and removed material in the form of microchips. Further cavitation is another phenomenon which assists the material removal. Cavitation collapse also leads to acceleration of abrasive particles [15]. Due to repeated tool impacts on the abrasive particles and cavitation, the tool wears. This tool wear is prominent once the tool material crosses its fatigue limit [12]. This phenomenon's predominantly occur in the zone-1 which is below the tool surface in the working gap. As fresh slurry is supplied continuously, the abrasives after striking in zone-1 move towards zone-2. Edge wear of tool has also been reported [7]. The vibrations of tool and constant supply of fresh slurry creates high pressure in zone-1. The previous abrasive particles which strike the glass surface are pushed to different sides of the tool. This resulted in entry of some abrasives towards lateral gap through zone-2.

During this movement of abrasives towards the lateral gap, the sharp edges of tool abrade in zone-2. The sharp edges of the tool became blunt after some time. Hence rounding of edges takes place. Simultaneously the abrasive particles came in contact at surface of the rounded edges of the vibrating tool, due to which

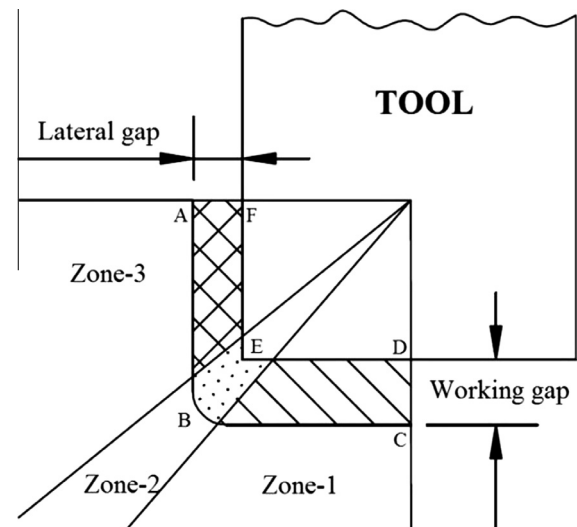


**Fig. 1.** Schematic showing the different zones of tool wear.

hammering phenomenon also occurred. Thus a combination of abrasion, cavitation and hammering occurs in the zone-2. The abrasive particles striking the round edges in zone-2 get deflected from the original path due to the pressure of slurry generated in zone-1.

These abrasive particles finally enters in zone-3 or the lateral gap. Literature reveals that friction alone was not the dominant factor of material removal; the rolling action of abrasives also accounts for the material removal [16]. As the lateral gap was very small, the abrasive motion in lateral gap is same with respect to workpiece walls and the tool. The abrasive collisions experienced by workpiece walls during rolling shall be experienced by the tool also. This implied that friction of abrasives and rolling action of abrasives was also responsible for tool wear during machining. Collectively, the combination of both the mechanisms implied a 3 body abrasion as the dominant mode of tool wear in zone-3 [17].

#### 4. Results and discussion

A one factor at a time approach was used to study the effect of step feed and abrasive size on the form accuracy of microchannels developed by WC and SS tool. In this study, the channels were machined by using three different abrasive sizes (1800#, 1000# and 800#) along with three different step feeds (5  $\mu\text{m}$ , 10  $\mu\text{m}$  and 15  $\mu\text{m}$ ). The experiments were conducted thrice and the mean value is presented in the Table 2. After a depth of 300  $\mu\text{m}$ , the tool profile and form accuracy was observed. The cross sectional views of the developed microchannels using different abrasive sizes are shown in Fig. 2a–f. It was observed that the width of microchannels increased when larger abrasive particles were used. This can be accounted due to the reason that the microchannel width is highly dependent upon the size of the abrasive particles exiting from the lateral gap. Larger the size of abrasive particle, larger will be the width of lateral gap. Hence, larger abrasives cause the microchannel profile to deviate from the intended form accuracy.

While USM, the tool face suffers from repetitive compressive stresses. The compressive stresses acting on the tool tip can be accounted due to three main interactions: tool-abrasive slurry, tool-abrasive slurry-workpiece and under extreme circumstances tool-workpiece interaction. As we increase the step feed from 5  $\mu\text{m}$  to 15  $\mu\text{m}$ , the compressive stresses acting on the tool face increase. This shall be due to above mentioned interactions. The kind of interaction exhibited mainly depends upon the depth of material removed on one pass of the tool. The material removal is highly dependent upon the abrasive size being used. Larger abrasive particle size results in larger craters over workpiece. These craters combine to form a new machined layer of definite depth. The depth of machined layer should be sufficient enough to incorporate a fresh laminar layer of abrasives between the working gap. But in case the material removal depth is insufficient than the step feed, the tool may come in contact with the workpiece in

next layer. So different step feeds had a different effect on the tool wear and the form accuracy.

From the cross sectional views of the developed microchannels shown in Fig. 2a–f it was observed that step feed and abrasive size are important parameters in deciding the form accuracy of the microchannel. It was observed that complete depth was obtained at a step feed of 5 and 15  $\mu\text{m}$ , but incomplete depths were obtained at 10  $\mu\text{m}$  using 1800# and 1000# size abrasive particles (Table 2). Thus, the step feed significantly affected the form accuracy.

In case of WC tool and using a step feed of 5  $\mu\text{m}$ , the hammering action of abrasives are mainly responsible for material removal. After striking the workpiece material, they are flushed away from the working gap without causing significant wear on the tool face. This can be seen from the complete depths obtained of the developed microchannels in Table 2. As the machining time involved is more in this case, the lateral wear on the tool edges is more and the microchannel profile obtained have generally rounded corners.

On the other hand machining by a WC tool at a step feed of 10  $\mu\text{m}$ , the developed microchannels using 1800# and 1000# were incomplete and more longitudinal wear was observed. The abrasive particles after striking the workpiece exited the working gap by rubbing the tool tip face leading to abrasion. A 3 body abrasion in this case was responsible for the reduced tool length (longitudinal wear) in WC and SS case illustrated in Fig. 3 [17]. A reduction of 21  $\mu\text{m}$  and 76  $\mu\text{m}$  in WC and SS tool was observed respectively when 1000# sized abrasive was used. Moreover the tool-abrasive-workpiece interaction was exhibited in this case.

Finally at a step feed of 15  $\mu\text{m}$ , microchannels of desired depth were formed. Lesser rounding of the microchannel corners was observed as shown in Fig. 2a and c. Complete depth of microchannels was obtained using the WC tool. In this case the tool also accompanied the material removal when 1800# and 1000# abrasive particles were used. The particles being small, were unable to remove sufficient material by the hammering action to compensate the next feed step. As the complete depth of the microchannels are formed (Table 2), it can be concluded that the material removal was also assisted by the tool-workpiece contact. The vibrating tool accompanies abrasive particles in the working gap when at peak position. When the tool came at its lower most position, it pierced the abrasive particles into the workpiece surface resulting in a contact between tool and workpiece. The striking tool causes development of radial and lateral cracks on the workpiece surface.

From Fig. 2b, d and f it was observed that incomplete depth was obtained when SS tool was used. On further investigation, a mushrooming effect of SS tool was observed in each case as shown in Fig. 4. The excessive compressive forces applied on the SS tool caused strain hardening of the tool surface. Thus, an increase in tool face diameter and reduction in length was generally observed. Further, the excessive localized heat generated at the tool face during machining was also responsible for the failure of SS tool.

**Table 2**  
Dimensions of the developed microchannels.

| S. no. | Abrasive size (#) | Step feed (in $\mu\text{m}$ ) | Microchannel dimensions using |                           |                           |                           |
|--------|-------------------|-------------------------------|-------------------------------|---------------------------|---------------------------|---------------------------|
|        |                   |                               | SS tool                       |                           | WC tool                   |                           |
|        |                   |                               | Width (in $\mu\text{m}$ )     | Depth (in $\mu\text{m}$ ) | Width (in $\mu\text{m}$ ) | Depth (in $\mu\text{m}$ ) |
| 1      | 1800              | 5                             | 688                           | 224                       | 643                       | 312                       |
| 2      | 1800              | 10                            | 674                           | 251                       | 629                       | 234                       |
| 3      | 1800              | 15                            | 690                           | 240                       | 625                       | 325                       |
| 4      | 1000              | 5                             | 668                           | 228                       | 659                       | 330                       |
| 5      | 1000              | 10                            | 683                           | 256                       | 653                       | 284                       |
| 6      | 1000              | 15                            | 775                           | 254                       | 637                       | 308                       |
| 7      | 800               | 5                             | 717                           | 288                       | 692                       | 323                       |
| 8      | 800               | 10                            | 701                           | 279                       | 695                       | 331                       |
| 9      | 800               | 15                            | 707                           | 319                       | 702                       | 325                       |

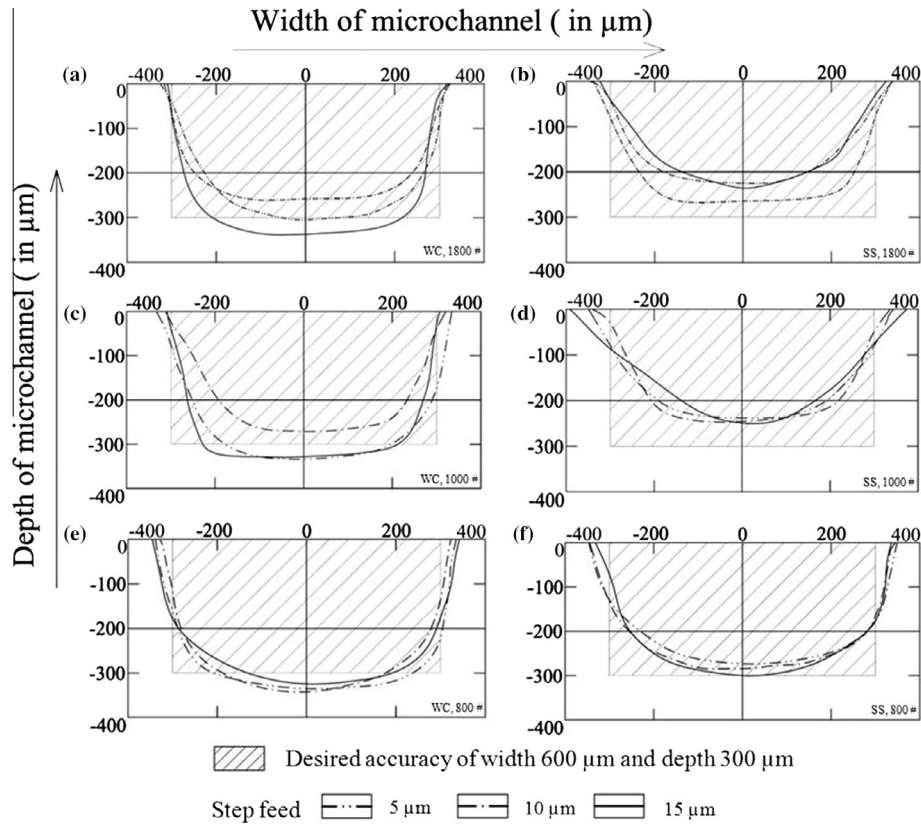


Fig. 2. Cross sectional view of the microchannels developed (a) WC tool, 1800#, (b) SS tool, 1800#, (c) WC tool, 1000#, (d) SS tool, 1000#, (e) WC tool, 800#, and (f) SS tool, 800#.

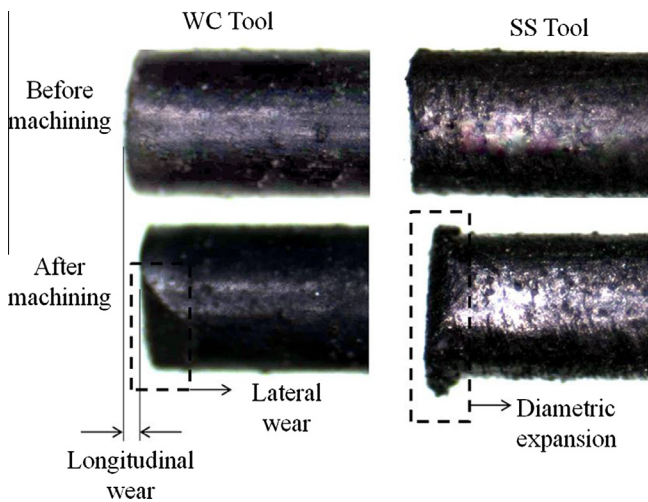


Fig. 3. WC and SS tool before and after machining with #1000 abrasive with step feed of 10 μm at 50× magnification.

| Step feed | Abrasive Size |       |      |
|-----------|---------------|-------|------|
|           | 1800#         | 1000# | 800# |
| 5         |               |       |      |
| 10        |               |       |      |
| 15        |               |       |      |

Fig. 4. Microscopic images (50×) of SS tool after experiments.

On the other hand, the high hardness of the WC tool made it withstand substantial compressive forces, even at a step feed of 15 μm.

To better understand the wear mechanism of SS and WC tool, a case study of microchannels developed at a step feed of 15 μm and abrasive size of 1000# can be considered for comparison.

The microchannels developed by using both the tools are shown in Fig. 5a and b. In both cases the total depth given to tool was 300 μm. The channel obtained by machining with SS tool had a near semicircular profile (Fig. 2d). An increased width overcut and reduced depth of microchannel are clearly visible in Figs. 5a

and 2d. Whereas in case of WC tool, slight tapered walls were obtained. Lesser stray cutting was observed on top surface of the microchannel developed by WC tool. The sectional view in Fig. 2c shows better replication of the dimensions of the WC tool on the glass workpiece (WC tool, 1000#, step feed 15 μm).

When the abrasive slurry flows below the vibrating tool, a number of particles experience direct impact with the vibrating tool. These impacts in turn, lead to strain hardening of the SS tool, consequently compression of top layer of the tool is observed. Such top

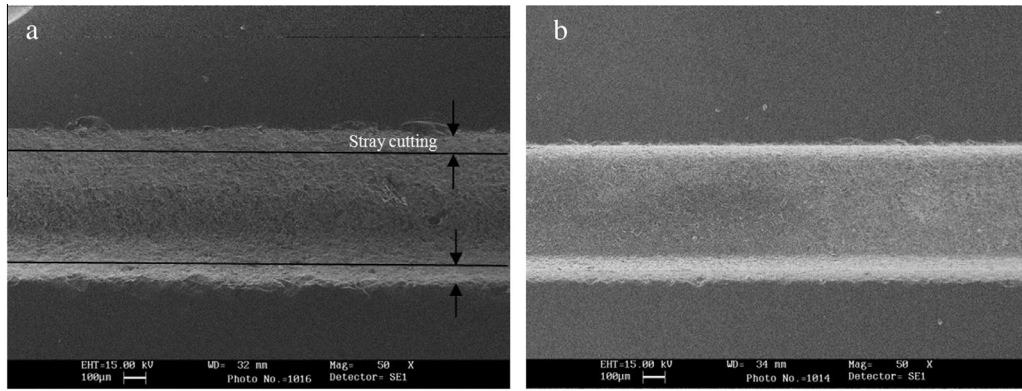


Fig. 5. Top view of microchannel machined by (a) SS tool, and (b) WC tool.

layer compression was reported earlier in case of SS 316 tool [14]. As the top layer compresses, the material (Fig. 6a–d) gets deformed laterally and flows. This results in an increase in the diameter of the tool. The material flow along lateral gap and the diametric expansion at a depth of 105  $\mu\text{m}$  is shown in Fig. 6a and c respectively. This deformed material along the lateral gap became an integral part of the tool and contributed to inaccuracy of the shape of micro channel. The dimensions of the microchannel along with schematic of tool tip formed after a depth of 105  $\mu\text{m}$  is shown in Fig. 6e. A taper of around 61° was observed in the microchannel wall. The final dia ( $d_f$ ) of the tool was 6.167% more than initial dia ( $d_i$ ).

By the deformation of the tool top surface, it can be inferred that some energy transmitted by the transducer assembly was not transferred to workpiece. This energy was consumed in

increasing tool wear and consequently form inaccuracy. This also reduced the material removal rate. At a depth of 210  $\mu\text{m}$ , it was observed that higher the machining depth, higher is the overcut (inaccuracy) as the channel width increased from 668  $\mu\text{m}$  to 732  $\mu\text{m}$  (Fig. 7a and b). A taper of 54° was observed at a depth of 210  $\mu\text{m}$ . The final diameter ( $d_f$ ) was found 10% more than the initial diameter ( $d_i$ ) at this depth. The magnitude of  $d_f$  is a function of machining time (machining depth) as well as the material properties.

The increased diameter further affected the shape of the channel being machined resulting in deterioration of the form accuracy. A clear deviation of the intended form of the microchannel could be seen vis-a-vis the tool schematic in Fig. 7a and b. As more and more depth was given, the SS tool behaved in an irregular manner. A significant amount of lateral overcut was

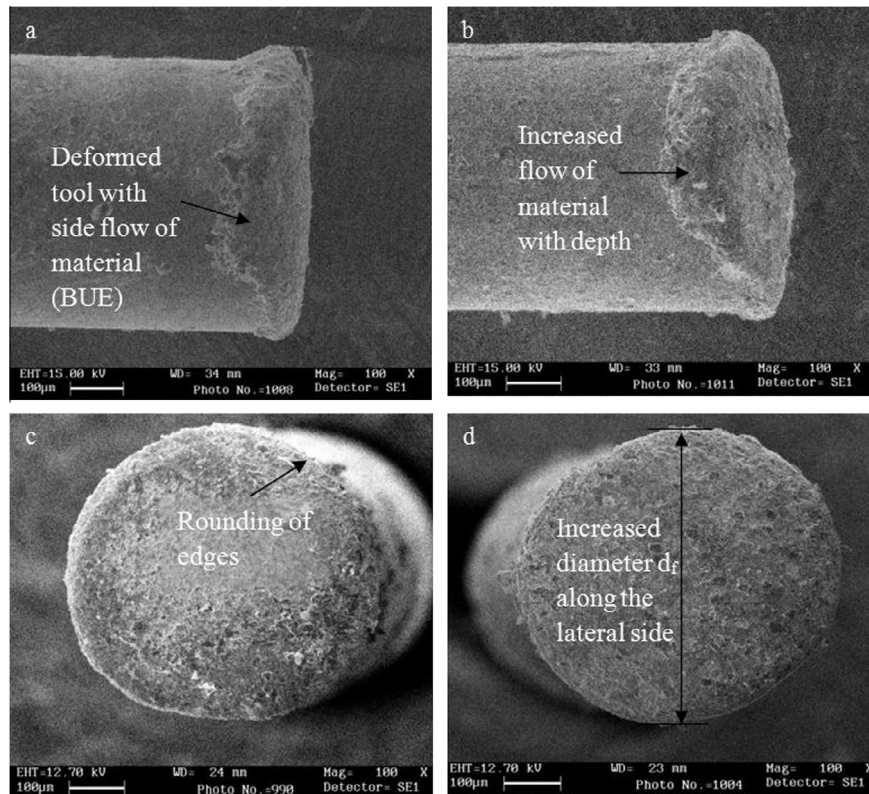


Fig. 6. Side view of the SS tool after machining at a depth of (a) 105  $\mu\text{m}$  and (b) 210  $\mu\text{m}$ , top view of the SS tool after machining at a depth of (c) 105  $\mu\text{m}$  and (d) 210  $\mu\text{m}$ .

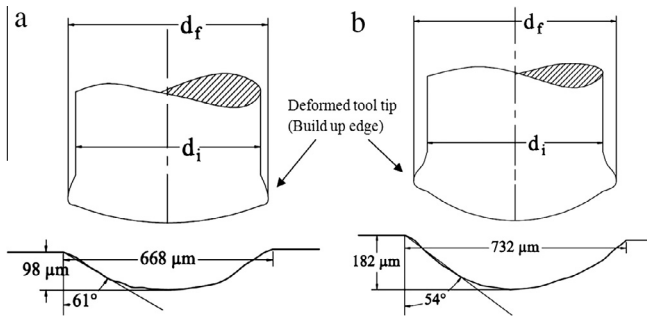


Fig. 7. Schematic of the profile formed after a depth of (a) 105  $\mu\text{m}$  and (b) 210  $\mu\text{m}$ .

observed due to the deformation of the top layers of the tool tip as evidenced in Fig. 5. This can be attributed due to the reason that at a depth of 210  $\mu\text{m}$  the scattered material after lateral deformation was dragged along the lateral gap (Fig. 6b and d). With increment in depth, this material, which is similar to a built up edge gets increased and participated in machining of the next layer. This apparent built up edge became a restriction to the movement of abrasive particles in the lateral gap as shown in Fig. 8a.

As constant pressure is exerted by the abrasives in working gap, the particles accumulate in between the built up edge and workpiece material. With more and more intake of abrasive slurry, the abrasives succeed in shearing of the tiny edges of the workpiece material along with it. As this action continues, the abrasive particles abrade the workpiece material generating an increased width and curved shape at the edges. The dotted line in Fig. 8a denotes the actual formed profile in glass workpiece. As this phenomenon is going continuously, some of the built up edge gets sheared from the tool. Finally at a depth of 300  $\mu\text{m}$ , a pointed edge

of the tool was formed. The tool edge became similar to that of a chisel shape as shown in Fig. 8b and c and the same shape is replicated on the microchannel in Figs. 2d and 5a. At the end, the width and depth of channel obtained from SS tool was 769 and 267  $\mu\text{m}$ . It can also be concluded that zone-2 decides the form accuracy of the microchannel in SS tool.

Contrary to this, from Fig. 9 it was observed that no top layer compression occurred in WC tool. Relatively WC tool has much higher hardness with respect to relatively tough SS tool, consequently higher energy could be transmitted to abrasive particles through impact and no diametric expansion occurred on the tool face. When the tool was given depth in next layer, the lateral gap formation started taking place. No side flow or lateral deformation was observed in case of WC tool.

From the observed wear in the SS and WC tool of above cases, the tool wear in microchannel development can be divided into a high wear region and a low wear region as shown in Fig. 10. Fig. 10 shows the top view of the tool which is moving in the forward direction. The side along the lateral gap is the high wear region and the side which does not encounter the lateral gap is the low wear region. High wear region exhibits zone-3 type wear which can also be seen in Fig. 9c, whereas the low wear region does not show the zone-3 of abrasion and rolling.

Unlike the SS tool in which form accuracy is decided by zone-2, the form accuracy in case of WC tool is decided by zone-3. As no diametric expansion of tool occurs in zone-1, this resulted in exit of abrasive particles first to zone-2 and then entering the zone-3 (Fig. 9a).

In the zone-3, the abrasive particles predominantly exhibit rolling. As the workpiece is given feed, the abrasive particles are dragged along the direction of the feed. Consequently, an intense interaction takes place between the three bodies – the tool body, the hard abrasive particles and the workpiece wall (Fig. 9a). As a

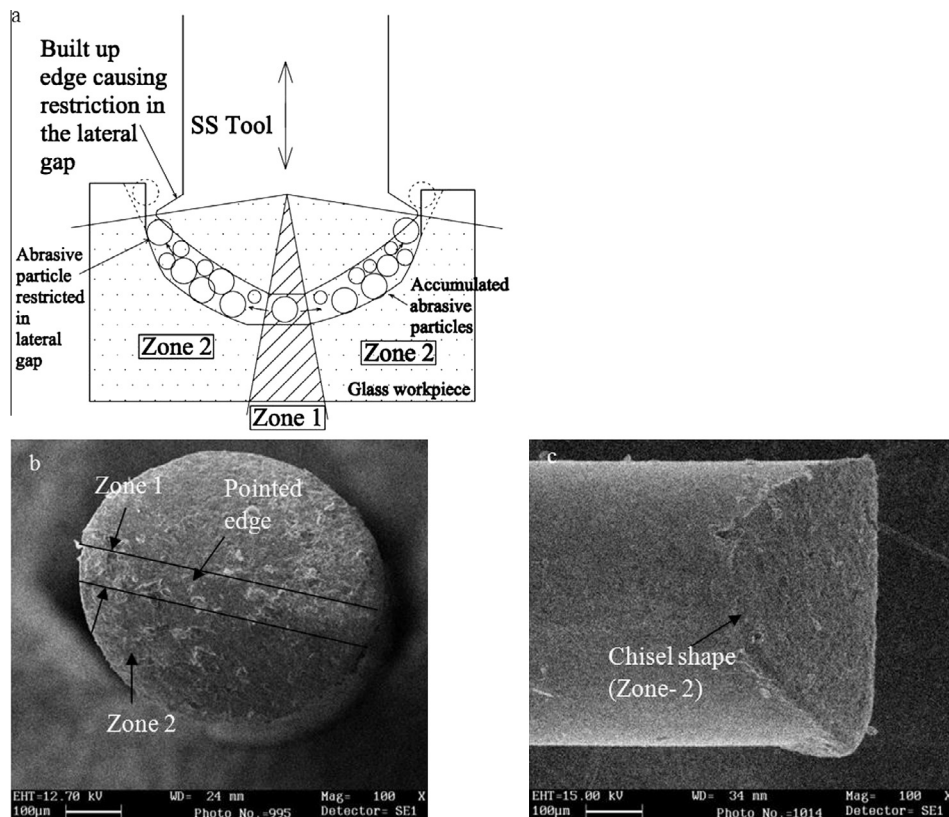


Fig. 8. (a) Schematic showing built up edge restricting the abrasive flow in the lateral gap in SS tool, (b) top view and (c) side view of the SS tool after a depth of 300  $\mu\text{m}$ .

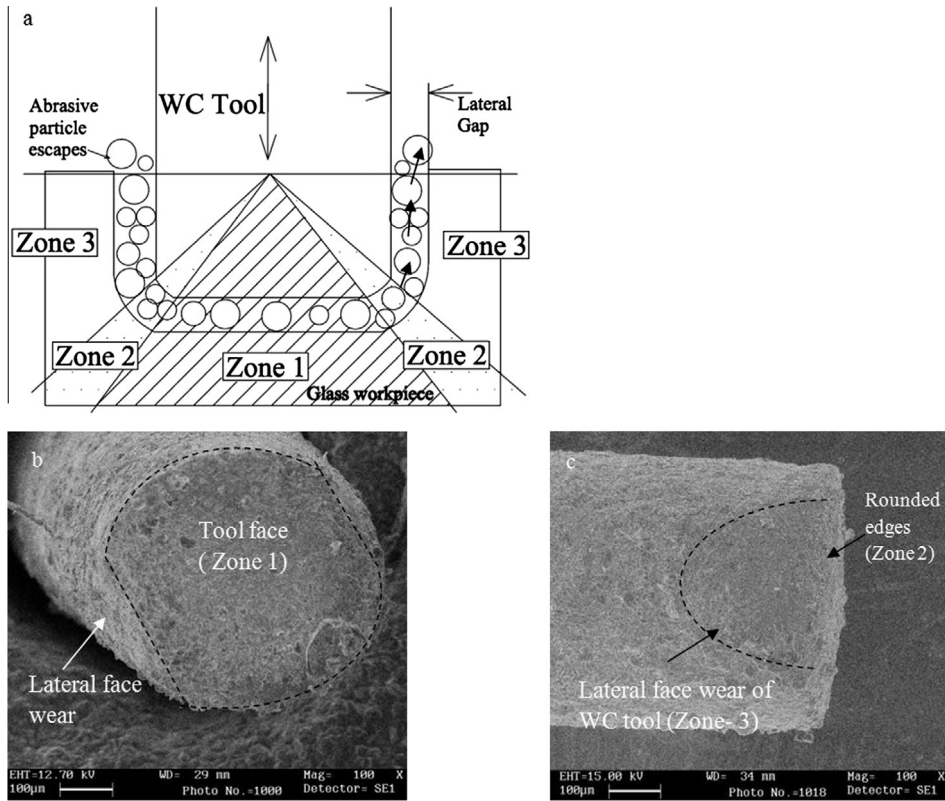


Fig. 9. (a) Schematic showing the abrasive exit in case of WC tool, (b) top view and (c) side view of the WC tool after a depth of 300 μm.

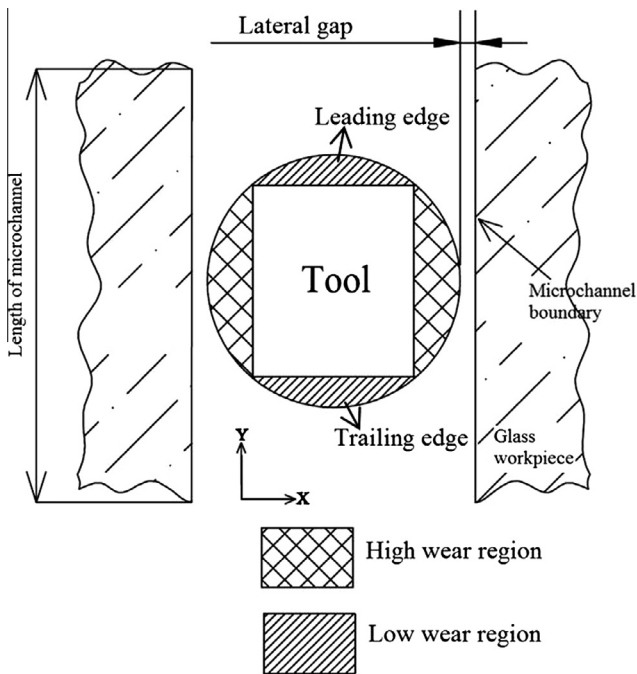


Fig. 10. Schematic showing top view of tool with high wear and low wear region.

result of this, both the walls, the external tool wall and the workpiece wall experience abrasion. The corresponding wear can be clearly seen in Fig. 9b and c. However, as the abrasives move up on the way to exit, the degree of interaction gets reduced. The abrasives at the bottom of the tool, get continuously impacted directly by the tool due to applied frequency. These abrasives loose

energy while moving upward through the tool-workpiece wall gap. Thus there will be a higher degree of wear near the bottom of the tool as compared to the top as evidenced by elliptical wear profile on the lateral face (Fig. 9c).

This results in a corresponding taper formation in the workpiece (microchannel) wall. This could be clearly evidenced by the tapered profiles of the fabricated microchannels as depicted in Fig. 2a, c, and e.

It is to be noted that, owing to the feed motion, the imparting abrasives do not find an easy exit from the leading face (advancing side) of the tool. Consequently, the resulting tool wear on this face shall be relatively lower than in the lateral region. These two high and low wear zones are shown schematically in Fig. 10. Further, the trailing face of the tool will not exert much pressure on the exiting abrasive particles and hence trailing face will also experience relatively low tool wear.

## 5. Conclusions

1. The relatively ductile nature of SS tool and lower hardness while comparison to WC tool, results in higher wear of SS tool making it unsuitable for layer by layer ultrasonic micromachining for precision application.
2. Microchannel width increased with use of larger abrasive particles. However the depth of the microchannel was mainly dependent upon the step feed.
3. The tool wear can be divided into three zones. The zone-1, existing in the working gap involves mainly hammering and cavitation action. Zone-2 prevails at the edges of the tool. The main wear mode here is hammering and abrasion. Zone-3 involves the lateral gap, where abrasion and rolling of abrasive particles is main mode of wear.

4. In WC tool the zone-3 wear is responsible for deciding the form accuracy. Whereas in SS tool, the zone-2 wear decides the form accuracy. The built up edge developed spreads the horizon of zone-2, resulting in dimensional inaccuracy.
5. The mechanism of strain hardening in SS tool is also responsible for affecting the form accuracy of developed microchannel. But in case of WC tool strain hardening is negligible compared to SS tool.

### Acknowledgement

The authors would like to express gratefulness to the Department of Science and Technology (DST), India, Grant no. SB/FTP/ETA/207/2012.

### References

- [1] T. Kohno, Y. Okazaki, N. Ozawa, K. Mitui, M. Omada, In process measurement and a workpiece-referred form accuracy control system (WORFAC): concept of the method and preliminary experiment, *Precis. Eng.* 11 (1) (1989) 9–14.
- [2] X.Q. Sun, T. Masuzawa, M. Fujino, Micro ultrasonic machining and its applications in MEMS, *Sensor. Actuat. A – Phys.* 57 (2) (1996) 159–164.
- [3] K. Egashira, T. Masuzawa, M. Fujino, X.Q. Sun, Application of USM to micromachining by on-the-machine tool fabrication, *Int. J. Electr. Eng. Mach.* (1997) 31–36.
- [4] K. Egashira, T. Masuzawa, Microultrasonic machining by the application of workpiece vibration, *CIRP Ann.-M* 48 (1) (1999) 131–134.
- [5] V. Jain, Investigations on development of microchannels using micro-ultrasonic machining Ph.D dissertation, Mech. and Indl. Engg. Dept., IIT Roorkee, 2012.
- [6] T.B. Thoe, D.K. Aspinwall, M.L.H. Wise, Review on ultrasonic machining, *Int. J. Mach. Tool. Manu.* 38 (4) (1998) 239–255.
- [7] M. Adithan, V.C. Venkatesh, Parameter influence on tool wear in ultrasonic drilling, *Tribol. Int.* 7 (6) (1974) 260–264.
- [8] M. Adithan, Tool wear studies in ultrasonic drilling, *Wear* 29 (1974) 81–93.
- [9] M. Adithan, V.C. Venkatesh, Tool wear mechanisms in ultrasonic drilling, *Wear* 34 (1975) 449–453.
- [10] M. Adithan, Tool wear characteristics in ultrasonic drilling, *Tribol. Int.* 14 (6) (1981) 351–356.
- [11] M. Komaraiah, P.N. Reddy, Relative performance of tool materials in ultrasonic machining, *Wear* 161 (1993) 1–10.
- [12] Z. Yu, C. Ma, C. An, J. Li, D. Guo, Prediction of tool wear in micro-USM, *CIRP Ann.-M* 61 (2012) 227–230.
- [13] Z.Y. Yu, K.P. Rajurkar, A. Tandon, Study of 3D micro-ultrasonic machining, *J. Manuf. Sci. E.-T. ASME* 126 (4) (2004) 727–732.
- [14] H. Xiao, Mechanism, Characteristics and Modeling of Micro Ultrasonic Machining, Ph.D Dissertation, University of Nebraska, Lincoln, 2007.
- [15] Y. Ichida, R. Sato, Y. Morimoto, K. Kobayashi, Material removal mechanisms in non-contact ultrasonic abrasive machining, *Wear* 258 (2005) 107–114.
- [16] C. Nath, G.C. Lim, H.Y. Zheng, Influence of the material removal mechanisms on hole integrity in ultrasonic machining of structural ceramics, *Ultrasonics* 52 (2012) 605–613.
- [17] I.D. Marinescu, W.B. Rowe, B. Dimitrov, I. Inasaki, *Tribology of Machining Processes*, William Andrew, USA, 2004.